THE ASTRONOMICAL JOURNAL VOLUME 106, NUMBER 5 NOVEMBER 1993

HIGH-SPEED PHOTOMETRIC OBSERVATIONS OF THE PULSATING DA WHITE DWARF GD 165

P. BERGERON,[1] G. FONTAINE,[1] P. BRASSARD, R. LAMONTAGNE, AND F. WESEMAEL

Département de Physique, Université de Montréal, C.P. 6128, Succ. A. Montréal, Québec, Canada, H3C 3J7
Electronic mail: (bergeron, fontaine, brassard, lamont, wesemael)@astro.umontreal.ca

D. E. WINGET, R. E. NATHER, P. A. BRADLEY, C. F. CLAVER, J. C. CLEMENS, S. J. KLEINMAN, AND J. PROVENCAL

Department of Astronomy and McDonald Observatory, University of Texas, Austin, Texas 78712
Electronic mail: (dew, nather, bradley, cfc, cclemens, sjk, judi)@astro.as.utexas.edu

J. T. MCGRAW

Department of Physics and Astronomy, University of New Mexico, Albuquerque, New Mexico 87131
Electronic mail: mcgraw@herschel.unm.edu

P. BIRCH AND M. CANDY

Perth Observatory, Bickley, Western Australia 6076

D. A. H. BUCKLEY

South Africa Astronomical Observatory, P.O. Box 9, Observatory 7935, South Africa
Electronic mail: dinob@saao.ac.za

P. TRIPE

Department of Astronomy, University of Cape Town, Rondebosch 7700, Cape Province, South Africa
Electronic mail: tripe@uctvax.uct.ac.za

T. AUGUSTEIJN

Astronomical Institute Anton Pannekoek, University of Amsterdam and Center for High Energy Astrophysics, Kruislaan 403, 1098 SJ Amsterdam, The Netherlands
Electronic mail: thomas@astro.uva.nl

G. VAUCLAIR[1]

Observatoire Midi-Pyrénées, 14 Avenue E. Belin, 31400 Toulouse, France
Electronic mail: vauclairg@fromp51.bitnet

S. O. KEPLER AND A. KANAAN

Instituto de Fisica, Universidade Federal do Rio Grande do Sul, 91500 Porto Alegre-RS, Brazil
Electronic mail: (kepler, kanaan)@if1.ufrgs.anrs.br

Received 1993 June 21

[1]Visiting Astronomer, Canada–France–Hawaii Telescope operated by the National Research Council of Canada, the Centre National de la Recherche Scientifique of France, and the University of Hawaii.

 0004-6256/93/106(5)/1987/13/$0.90

ABSTRACT

New high-speed photometric observations of the pulsating DA white dwarf GD 165 are presented. The Fourier spectrum of the light curve of GD 165 exhibits two main regions of power at 120 and 193 s. The presence of a high-amplitude long period mode near ~1800 s reported by Bergeron and McGraw is not confirmed by these new observations. Light curves obtained with the Canada–France–Hawaii Telescope reveal previously undetected low-amplitude harmonic oscillations. Observations with the Whole Earth Telescope are used to resolve the two principal regions of power. The 120 and 193 s peaks are shown to be multiplets composed of at least three, and possibly five frequency components. The most likely explanation is that these two peaks correspond to nonradial gravity modes with different values of the radial order k and with $l=1$ or 2 split into $2l+1$ components by slow rotation. The frequency differences observed between the three dominant components of each peak are consistent with equal spacing, but a slight asymmetry in spacing cannot be totally ruled out at this stage. They suggest a rotation time scale of the order of 4.2 days. Within a peak, power is not distributed evenly or symmetrically among the three frequency components, particularly for the 193 s mode. Consequently, a simple interpretation in terms of geometric effects (inclination of the pulsation axis with respect to the line of sight) cannot be invoked here. The tentative identification of modes with $l=1$ or 2 is used to constrain the hydrogen layer mass in GD 165. In particular, the 120 s pulsation mode has a period sufficiently short that useful limits can be derived on this quantity. Using recent adiabatic pulsation calculations and new determinations of the atmospheric parameters of GD 165, it is found that $\mathscr{M}(\mathrm{H})/\mathscr{M}_{*} \gtrsim 10^{-3.7}$ or $\gtrsim 10^{-6.4}$ if the 120 s pulsation is a mode with $l=1$ or 2, respectively.

1. INTRODUCTION

The star GD 165 (WD 1422+095, L1124−10, LP 500−17, LTT 14236) was discovered to be a variable DA white dwarf, or ZZ Ceti star, by Bergeron & McGraw (1990). The variability of this object had been predicted from a determination of the atmospheric parameters, since a detailed comparison of high signal-to-noise spectroscopy with model atmosphere calculations had indicated that the derived temperature of GD 165 fell inside the ZZ Ceti instability strip where all pulsating DA stars are found. In the first photometric observations of GD 165, the light curve of GD 165 appeared to be dominated by extremely long periods (> 1000 s) and to have changed dramatically on a time scale of only two days. The discovery runs were all obtained with a single-channel aperture photometer, however, and although the quality of the data was sufficient to assess the variability of GD 165, Bergeron & McGraw (1990) pointed out that additional work would be required to determine its period structure. We report here the results of three independent sets of high-quality observations obtained subsequently.

Our first series of followup observations were obtained at the Mount Bigelow Observatory in early 1990 with LAPOUNE, the Montréal three-channel photometer. The observations are reported in Sec. 2. We also took advantage of an observing run at the Canada–France–Hawaii Telescope (CFHT) in 1990 April, with the same instrument, to examine the light curve of GD 165 at very high signal-to-noise ratio (Sec. 3). Finally, due to its relative brightness ($V=14.3$) and its near equatorial position, GD 165 was selected as the secondary target during the Whole Earth Telescope (WET) (Nather 1989; Nather *et al.* 1990; Winget 1991) campaign of 1990 May. These last two sets of observations are largely complementary; the CFHT data show unprecedented sensitivity to the presence of low-amplitude modes, while the WET data provide high temporal resolution which reveals frequency splitting of the dominant pulsation modes in the Fourier domain. The results of our analysis of the WET data are presented in Sec. 4. The three data sets are combined and analyzed in Sec. 5. From these, we obtain constraints on possible mode identification for the dominant pulsation modes in GD 165 and infer interesting limits on the hydrogen layer thickness in that star. This is discussed in Sec. 6. A brief conclusion is also presented in the last section.

2. OBSERVATIONS OF GD 165 AT MOUNT BIGELOW

Our first follow up observations of GD 165 were obtained on 1990 January using LAPOUNE attached to the Mount Bigelow 1.6 m telescope. This photometer is equipped with Hamamatsu R647-04 photomultipliers and allows continuous monitoring of the target object, a comparison star, and the sky background. All observations were obtained using 10 s integrations, and white light photometry was used throughout to maximize the signal-to-noise ratio. Because the guiding was performed manually, we used a fairly large aperture (28″) for all three channels. Details of our observing procedure with this instrument and data reduction are described in Fontaine *et al.* (1991). The journal of observations is presented in Table 1.

We present in Fig. 1 the Fourier *amplitude* spectra (i.e., the square root of the more standard *power* spectra) for the four observing runs at Mount Bigelow. The regions from 11 mHz out to the Nyquist frequency (50 mHz) are consistent with noise and are thus not displayed here. The Fourier spectra of GD 165 exhibit two main regions of power at 8.3 mHz (120 s) and 5.2 mHz (193 s). Another peak near 4 mHz (250 s) is also seen in the last run and is confirmed by subsequent observations (see below). The amplitudes of the 120 and 193 s peaks are highly variable;

TABLE 1. Journal of observations.

Run Name	Telescope	Date (UT)	Start (UT)	Length (s)
JTM-0037...	Mt. Bigelow 1.6 m	1990 Jan 26	10:31:35	5630
JTM-0042...	Mt. Bigelow 1.6 m	1990 Jan 28	8:08:53	10860
JTM-0044...	Mt. Bigelow 1.6 m	1990 Jan 29	9:21:14	12490
JTM-0047...	Mt. Bigelow 1.6 m	1990 Jan 30	8:45:49	14420
FBV-004....	CFHT 3.6 m	1990 Apr 1	11:35:37	12720
FBV-006....	CFHT 3.6 m	1990 Apr 2	10:23:22	17100
PAB-0037...	McDonald 0.9 m	1990 May 21	7:56:30	7290
S5086.....	SAAO 0.8 m	1990 May 23	17:41:00	21610
RA155.....	Itajuba 1.6 m	1990 May 24	22:23:20	8800
S50926.....	SAAO 0.8 m	1990 May 25	17:10:40	17870
RA159.....	Itajuba 1.6 m	1990 May 25	22:05:50	8910
S5095.....	SAAO 0.8 m	1990 May 26	17:59:40	20690
RA165.....	Itajuba 1.6 m	1990 May 27	1:08:40	13290
SJK-0092....	ESO 1.0 m	1990 May 27	4:47:30	10280
CFC-0048...	Mauna Kea 0.6 m	1990 May 27	6:00:00	2540
CFC-0049...	Mauna Kea 0.6 m	1990 May 27	6:51:30	21220
S5097.....	SAAO 0.8 m	1990 May 27	17:57:01	14320
PAB-0043...	McDonald 0.9 m	1990 May 28	3:09:30	20290
S5120.....	SAAO 0.8 m	1990 May 28	17:25:32	20300
CFC-0051...	Mauna Kea 0.6 m	1990 May 29	6:00:00	25820
JCC-0155...	Perth 0.6 m	1990 May 29	11:02:00	25780
S5122.....	SAAO 0.8 m	1990 May 29	18:36:01	7000
PAB-0046...	McDonald 0.9 m	1990 May 30	3:10:00	11800
CFC-0052...	Mauna Kea 0.6 m	1990 May 30	5:59:30	19060
S5124.....	SAAO 0.8 m	1990 May 30	17:30:01	13310
S5125.....	SAAO 0.8 m	1990 May 30	22:40:01	8000

this suggests that each mode is composed of at least two unresolved frequency components. During the time span of the observations, the amplitude of the 120 s peak varied from about 0.8% down to 0.25%. The 193 s peak reached maximum and minimum amplitudes roughly at opposite phase compared to the 120 s peak, but with comparable amplitudes ranging from $\sim$0.15% to 0.5%. The amplitude spectrum obtained on the first night is almost identical to that observed 4 nights later. If beating between unresolved frequency components is responsible for the amplitude modulation, our results indicate that the beat period is of the order of 4 days. In principle, the beat period could be less than this ($\sim$4 days divided by an integer), although it is possible from Fig. 1 to rule out beat periods of 2 days or less. Hence, both the 120 and 193 s peaks have similar beat periods which must be of the order of $\sim$4 days.

Although both the 120 and 193 s peaks were present in one of the light curve (and Fourier transform) displayed in Bergeron & McGraw (1990), none of the other peaks reported in that analysis are observed here. It is very likely that those additional peaks were caused by atmospheric transparency and sky background variations which are difficult to evaluate when the observations are obtained with a single-channel photometer. In particular, the long-period dominant mode near 1800 s reported by Bergeron & McGraw (1990) is not seen in the current data set. Such a long period taken together with the apparent temperature of GD 165 near the blue edge of the ZZ Ceti instability strip was a puzzle (see Daou *et al.* 1990) as it represented a clear exception to the observed period–luminosity trend in ZZ Ceti stars (Winget & Fontaine 1982). Our current estimate of the temperature of GD 165 using properly time-averaged spectroscopy is $T_{\rm eff}$=13 300 K, which, combined with our new photometric observations of GD 165, actually strengthens this period–luminosity relation in which hotter objects tend to have shorter dominant periods.

3. HIGH SIGNAL-TO-NOISE OBSERVATIONS AT THE CFHT

GD 165 was scheduled to be observed with the WET network during the campaign of 1990 May. Unfortunately, no large aperture telescopes were part of the network during that campaign. However, we did take advantage of the availability of the Canada–France–Hawaii 3.6 m telescope on Mauna Kea during the earlier WET campaign of 1990 April (mostly dedicated to G117-B15A; see Kepler *et al.* 1991) to search for low-amplitude pulsations in GD 165. The star was observed on two consecutive nights using LAPOUNE. As before, white light photometry was used with 10 s integrations, and a 10″ aperture was used in all channels. Accurate automatic offset guiding was provided by the CFHT bonnette. The photometric quality of the nights was truly exceptional, as could be ascertained from the constant comparison star. The journal of our observations is reported in Table 1.

A segment of the light curve obtained on the first night is reproduced in Fig. 2. Complex constructive and destructive patterns are clearly seen in the light curve as a result of the interaction between the various pulsation modes

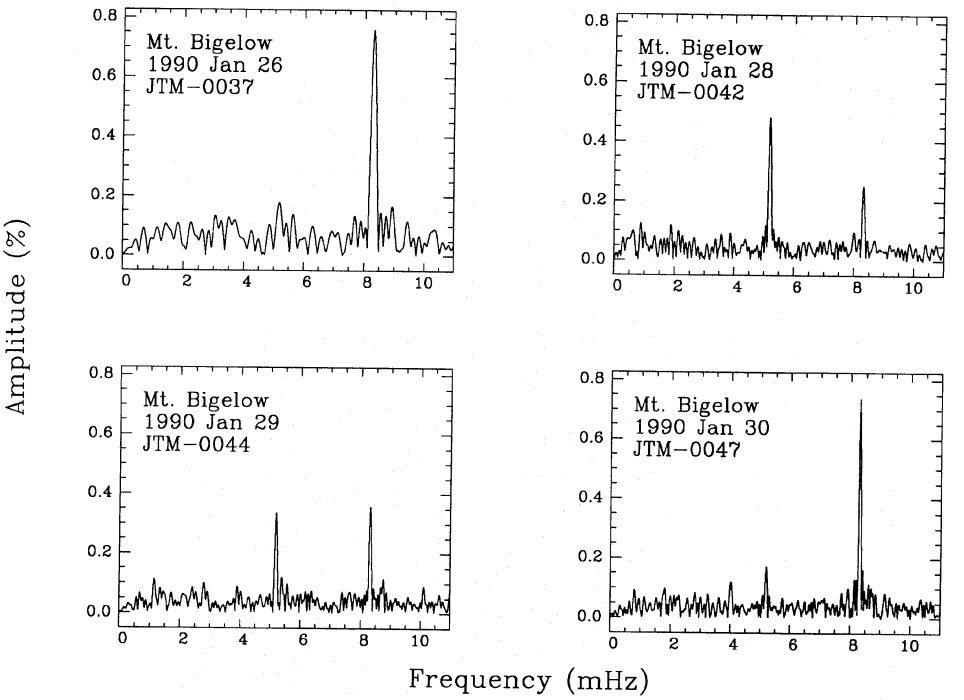

FIG. 1. Amplitude spectra of GD 165 derived from the four light curves obtained with the 1.6 m telescope at Mount Bigelow, expressed in terms of a percentage of the mean intensity of the star. For comparison, all spectra are shown on the same scale. The region from 11 mHz out to the Nyquist frequency is consistent with noise and is not displayed here.

present. As shown below, the period structure was then dominated by the same 120 and 193 s pulsations as before, but this time, with comparable amplitudes.

The amplitude spectra of both CFHT runs are displayed in Fig. 3. Although, at best, only three regions of power were observed with the relatively small aperture of the Mount Bigelow telescope (see also Sec. 4), the remarkable high signal-to-noise ratio of the light curves obtained at the CFHT revealed at least 8 significant excited pulsations. Of course, these low-amplitudes oscillations could be uncovered only because of our use of the large aperture of the CFHT which reduced the noise to an exceptionally low value of $\sim$0.25 mmag or less. Examination of Fig. 3 indicates that some of these pulsations were observed on both nights while others were seen on one night only, again suggesting some beating in these peaks also. The individual

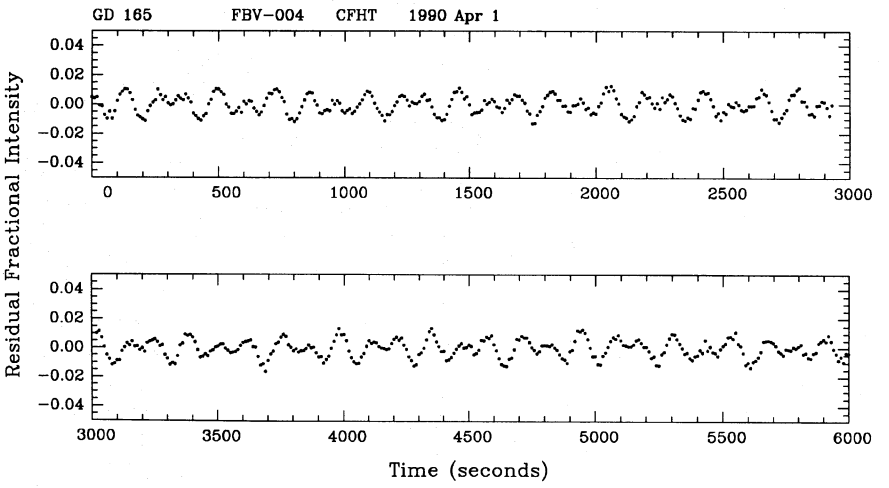

FIG. 2. Segment of the light curve of GD 165 obtained on 1990 April 1 with the CFHT, expressed in residual fractional intensity. Each data point represents a 10 s integration.

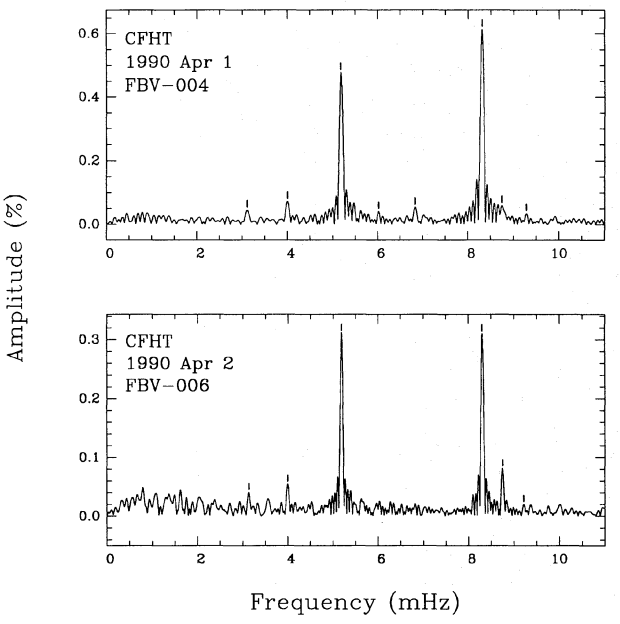

FIG. 3. Low-frequency part of the amplitude spectra of GD 165 obtained at the CFHT, expressed in terms of a percentage of the mean intensity of the star. Note that the vertical scale of the lower panel is expanded. The individual peaks are indicated by tick marks. The region from 11 mHz out to the Nyquist frequency is consistent with noise and is not displayed here.

peaks identified are marked on Fig. 3 and reported in Table 2 together with the corresponding amplitudes. A comparison of the amplitude spectra obtained at the CFHT with those obtained at Mount Bigelow (Fig. 1) indicates that the 120 and 193 s peaks were in a slightly different phase of beating. Indeed, when GD 165 was observed at the CFHT the amplitude of both peaks varied more or less in phase, with comparable amplitudes ranging from 0.3% to 0.6%.

The importance of our discovery of low-amplitude modes in GD 165 cannot be overemphasized because our ability to constrain uniquely the internal structure and exploit the full potential of asteroseismology for that star depends on the number of linearly independent pulsation modes detected. Note that some of the low-amplitude harmonic oscillations uncovered here are not necessarily linearly independent pulsation modes. For example, the small peak at $\sim$3.12 mHz corresponds to the frequency difference between the two dominant peaks and is most probably the consequence of the nonlinear superposition of these two modes and not an independent pulsation mode. The amplitudes of such nonlinear peaks relative to those of basic modes contain very important information as to the geometry of the temperature waves which characterize g-mode pulsations in white dwarfs. This information is of fundamental importance for mode identification. We make no attempt in the present paper to decipher completely the light curve of GD 165 (especially in the light of our CFHT observations), as the necessary theoretical tools are only currently being developed. The most promising progress in this area appears to be along the lines of attack being explored by Brassard *et al.* (1993a) and Brassard *et al.* (1993b).

TABLE 2. Observed periods at the CFHT.

FBV-004			FBV-006		
Frequency (mHz)	period (s)	Amplitude (%)	Frequency (mHz)	period (s)	Amplitude (%)
3.11.....	321.21	0.045	3.13.....	319.34	0.040
4.00.....	249.73	0.073	4.00.....	250.11	0.053
5.18.....	192.73	0.480	5.19.....	192.50	0.311
6.01.....	166.15	0.041	...	...	...
6.83.....	146.40	0.054	...	...	...
8.31.....	120.37	0.613	8.31.....	120.37	0.310
8.75.....	114.32	0.059	8.75.....	114.24	0.081
9.28.....	107.71	0.035	9.21.....	108.49	0.020

4. HIGH TEMPORAL RESOLUTION OBSERVATIONS OF GD 165 WITH WET

4.1 Observations

The primary target of the 1990 May campaign was GD 358, a DB variable, a brief summary of the analysis of which has been reported by Winget (1991). After the amplitude spectrum of GD 358 has finally been resolved into its frequency components, attention was then turned to GD 165, the secondary target of the campaign. Unfortunately, since we were close to the end of the campaign, some observing sites with critical longitudinal locations were no longer part of the network, leaving important gaps in the data string. Furthermore, uncooperative weather in Australia produced even more undesirable aliases in the derived window function, such as those illustrated in Fig. 1 of Nather *et al.* (1990). As shown below, the coverage of the observations was nevertheless sufficient to extract useful information on GD 165.

The journal of observations of the 1990 May campaign on GD 165 is summarized in Table 1 in order of increasing starting time (UT) of the individual runs. The total time span of our observations is 233 h (35% of which were covered) which yields a frequency resolution (FWHM) of $\sim$1.2 μHz. The individual runs are also displayed in Fig. 4 in terms of their location and time coverage. Most observations were obtained with 2-channel photometers, except at Perth, Australia where the Montréal 3-channel photometer was used. The data were reduced following the standard procedure outlined in Nather *et al.* (1990) and Winget *et al.* (1991).

4.2 The Complete Fourier Transform

The complete Fourier transform of the entire data string from the WET campaign has been computed following the procedure outlined in Nather *et al.* (1990) in which the Fourier spectra of the individual runs are added together into real and imaginary arrays whose size and resolution are determined from the total length of the WET run.

The amplitude spectrum of the complete data set is displayed in Fig. 5. Again, the region from 10 mHz out to the Nyquist frequency is consistent with noise and is not dis-

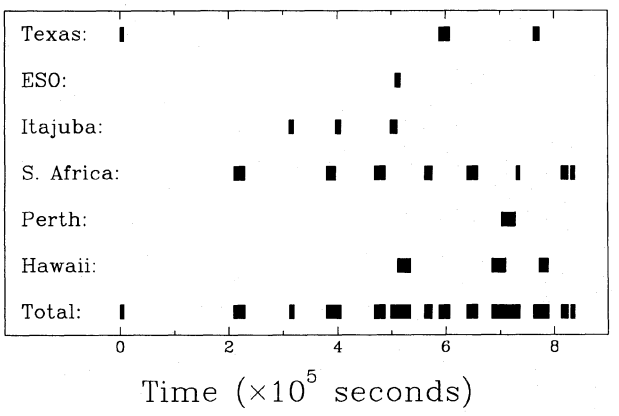

FIG. 4. Coverage of the Whole Earth Telescope during the 1990 May campaign on GD 165. The different segments represent the length of each run at various observing sights. The total coverage of the WET campaign on GD 165 is shown at the bottom.

played here. Characteristically, the noise increases with decreasing frequency, until the turnover at very low frequencies which is the direct result of our correction procedure for atmospheric extinction. Three regions of power observed in the CFHT data set are seen in the WET data as well, namely the peaks at 4.0, 5.2, and 8.3 mHz (250, 193, and 120 s). The amplitudes of these peaks are approximately 0.10%, 0.25%, and 0.53%, respectively. Since the noise level of the WET data on GD 165 is approximately 0.04% (for frequencies greater than ~3 mHz), most of the low amplitude modes observed at the CFHT could not be detected here.

4.3 Analysis of the Individual Frequency Components

We have derived the window function of the entire WET run by taking the Fourier transform of a single sinusoid sampled in the exact same manner the data were

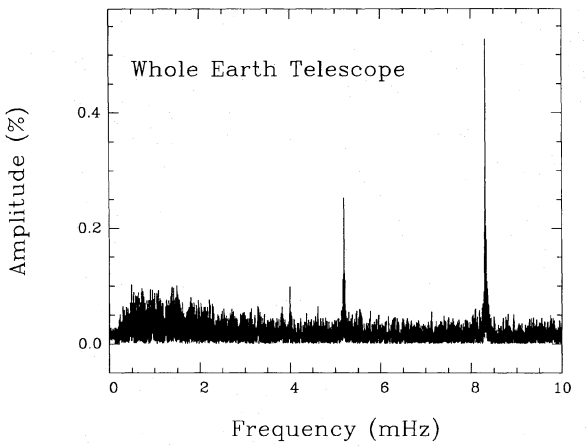

FIG. 5. Low-frequency part of the amplitude spectrum obtained from the entire data set of the WET campaign on GD 165. Once again, the region from 10 mHz out to the Nyquist frequency is consistent with noise and is not displayed here.

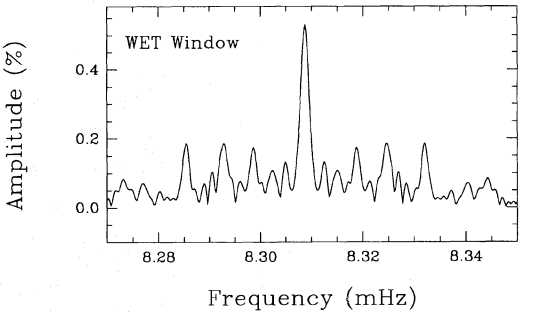

FIG. 6. Window function of the entire WET run obtained by taking the Fourier transform of a single sinusoid (with a period of 120.36 s) sampled in the exact same manner the data were gathered.

obtained. As discussed by Winget *et al.* (1991), this method is somewhat less conventional than the usual window function obtained by transforming a sampled signal of frequency 0 and amplitude 1, but possesses the same properties, with the advantage that the amplitudes of the window function can be compared directly with those obtained from the real observations. Furthermore, it allows the possibility of taking into account more than one frequency component, if present (also called spectral synthesis by others).

The window function of the 120 s peak is displayed in Fig. 6; the window function of other peaks can be obtained directly by simply applying a frequency shift to Fig. 6. Many sidelobes resulting from gaps present in the data string (see Fig. 4) are clearly visible in the window function, in contrast to the much cleaner window functions obtained for GD 358 (Winget 1991) or PG 1159−035 (Winget *et al.* 1991), but somewhat comparable to that of G29-38 (Winget *et al.* 1990). Therefore, our only hope to be able to decipher the fine structure present in each region of power of GD 165 is that the different frequency components are not aligned with any of these sidelobes. This problem of identification will be further exacerbated if the amplitudes of these components are small. The Fourier transforms of the 120 and 193 s peaks are displayed in Figs. 7 and 8, respectively. These results are discussed in turn.

4.3.1 The 120 s peak

The amplitude spectrum of the 120 s peak (Fig. 7) exhibits, at first glance, only one single frequency component. However, the detailed comparison with the window function (shown as a dotted line) reveals two more frequency components very close to the main peak. These components (identified by long tick marks) are located near the minima of the window function and there is therefore no doubt about their existence. The short tick marks indicate the location corresponding to twice the observed frequency spacing expected from the rotational splitting (see Sec. *4.4*) of the $2l+1$ (with $l=2$) orbital components. The amplitudes of these components, if any, are relatively small. The amplitudes and periods of the individual com-

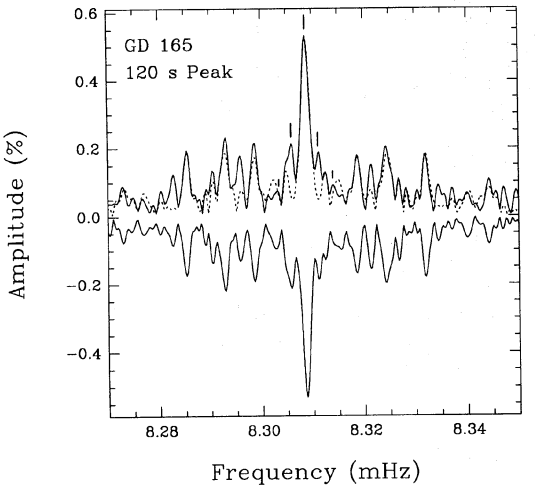

FIG. 7. Amplitude spectrum of the 120 s peak. The solid curve at the top is the Fourier transform of the entire WET data set, while the dotted curve is a reproduction of the window function displayed in Fig. 6. The three individual frequency components are indicated by long tick marks; the short tick marks correspond to twice the frequency spacing of the secondary components. The curve at the bottom (*vertically reversed*) is the Fourier transform (window function) obtained from a sum of the three individual components of Table 3.

ponents are usually extracted from the Fourier transform by first fitting the amplitude and phase of the dominant component with a sine wave function at the observed period of that component. Then, by subtracting from the data string a sine wave function with the corresponding period, amplitude, and phase, it is generally possible to unveil the weaker components. These components are then fitted in a similar manner until the Fourier spectrum obtained from the entire data string, *with all the frequency components subtracted*, is consistent with noise. Although this procedure works perfectly when the components are well resolved, the derived amplitudes may be inaccurate when the window function of one peak interferes with the amplitude of another peak.

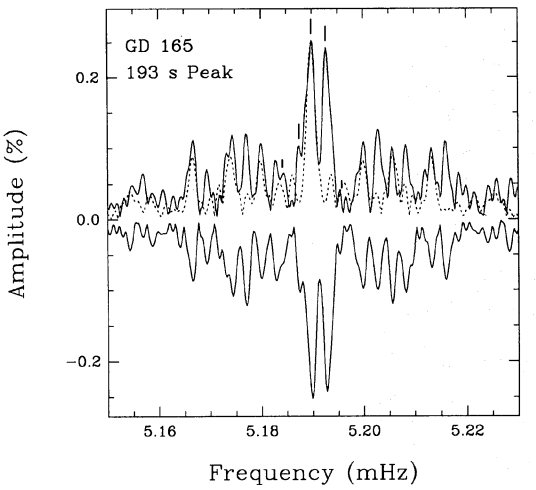

FIG. 8. Same as Fig. 7 for the 193 s peak.

The window function of the 120 s region (Fig. 7) shows that the main peak interferes slightly with the secondary peaks. Consequently, when the procedure described above is used to analyze the data, the amplitudes of the window function computed from the sum of the individual components (with corresponding periods, amplitudes, and phases) come out too large as compared with the observed amplitudes. Instead, we have relied upon a different procedure and fitted the three components *simultaneously*. This procedure ensures that the amplitude of the individual components come out correctly.

The periods and amplitudes of the three components of the 120 s peak are reported in Table 3. A Fourier transform obtained from the sum of the individual components (with corresponding amplitudes and phases taken into account) is shown in Fig. 7 as a reversed image. Most details in the observed spectrum are quite well reproduced, indicating that the frequency components and amplitudes have been extracted properly from the data set. The small differences observed are entirely consistent with noise, which is of course not present in the calculation of the reconstructed window function.

4.3.2 The 193 s peak

The Fourier transform of the 193 s peak is displayed in Fig. 8. There are at least two frequency components present in this region with nearly equal amplitudes. However, a detailed comparison of the amplitude spectrum with the window function of a single sinusoid indicates that there is also a third component in the spectrum with a much smaller amplitude and lower frequency than the other two peaks. This third peak is located near the minimum of the window function of the middle component (see Fig. 8) and although not displayed here, it also coincides with a minimum of the window function of the high frequency component of the triplet. This low-frequency peak can also be observed more clearly by subtracting the two other frequency components from the data set. As before, these three peaks are identified by long tick marks and the location corresponding to twice the frequency spacing is indicated by short tick marks.

For the same reasons mentioned above, we have fitted the amplitudes and phases of all peaks simultaneously. The periods, amplitudes, and phases are given in Table 3. Again, the Fourier transform obtained from the sum of these individual components (the window function) is shown in Fig. 8 as a reversed image. Most features seen in the observed data are well reproduced in the reconstructed Fourier transform. The small differences observed are entirely consistent with noise present in the data.

4.3.3 The 250 s peak

The remaining region of power in the complete Fourier transform (Fig. 5) is located near 250 s. A closer look at this region reveals the presence of at least one strong peak at 250.1864 s (3.9970 mHz) with an amplitude of about

TABLE 3. Peaks in the power spectrum obtained with the WET.

120 s Peak			193 s Peak		
Frequency (mHz)	Period (s)	Amplitude (%)	Frequency (mHz)	Period (s)	Amplitude (%)
8.3058.....	120.3972	0.153	5.1874.....	192.7716	0.058
8.3087.....	120.3558	0.506	5.1900.....	192.6831	0.226
8.3111.....	120.3212	0.128	5.1927.....	192.5770	0.214

0.1%. It was not possible to perform the same detailed analysis described above for this peak because the noise is comparable to the signal. We have tried to subtract from the data set the first frequency component, and possibly found a second peak with a period of 250.6797 s (3.9892 mHz) and an amplitude of about 0.06%. However, the results are quite uncertain and higher signal-to-noise data at a comparable frequency resolution will be required to analyze this region of power properly.

4.4 Interpretation of the Frequency Spacings

It is now possible to use the results given in Table 3 to draw some conclusions about the period structure of GD 165. In the following, we will assume that the 120 and the 193 s peaks consist of only three components, and assign a value of $m=0$ (the azimuthal quantum number) to the central component. Furthermore, we adopt the convention of Unno *et al.* (1989) where the higher frequency component is assigned a $m=+1$ value.

The measured frequency spacings between the frequency components of the 120 s peak are slightly different: The spacing between the $m=+1$ and the $m=0$ components is $\delta\nu_{m=+0,1}=2.4$ μHz, while that between the $m=0$ and $m=-1$ components is $\delta\nu_{m=0,-1}=2.9$ μHz. However, this difference is not significant if one considers that the resolution of the spectrum (FWHM) is only 1.2 μHz. Therefore, these results are consistent with an equal frequency spacing. Indeed, the analysis of Sec. *4.3.1* can be repeated by *assuming* an equal spacing without affecting the results. Similarly, we find for the 193 s peak a spacing of $\delta\nu_{m=+1,0}=2.7$ μHz and $\delta\nu_{m=0,-1}=2.6$ μHz which is entirely consistent with an equal spacing.

If we take an average of the frequency spacing of each peak, we arrive at the same value of $\delta\nu=2.65$ μHz. Although it may be tempting to conclude from this that both dominant modes belong to the same l sequence because their (presumably) rotationally-split m components show the same frequency spacing, it is well to remember that this is a result of nonradial pulsation theory which is valid *only* in the limit of high radial order modes (large values of k). The modes of interest in GD 165 are most certainly very low radial order modes (because their periods are short), and the asymptotic theory is inadequate in that regime. Figure 18 of Brassard *et al.* (1992) explicitly shows how the rotation coefficient C_{kl} varies as a function of k in ZZ Ceti star models. Thus, the coincidence between the average period spacings for the two dominant modes is most probably fortuitous. Nevertheless, the available data *do* suggest that each region of power represents excited modes characterized by a given value of the harmonic index, l, in which stellar rotation has removed the orbital degeneracy of the $2l+1$ components. Moreover, since both the 120 and the 193 s peaks are multiplets composed of at least three equally-spaced components, it is tempting to identify each peak with an $l=1$ mode, although the limited signal to noise of the current data sets and possible geometrical effects (see Sec. 5) prevent us from ruling out completely higher values of l. Furthermore, the frequency resolution is not sufficient to ensure that we are indeed dealing with identical pulsation modes for each peak. We have therefore relied upon the data sets of the other runs from Mount Bigelow and the CFHT to increase the time baseline, and hence the frequency resolution.

5. COMBINING ALL DATA SETS

The frequency resolution of the Fourier transform is significantly increased if all observations are considered simultaneously. The observations cover a time span of nearly 10^7 s which yield a frequency resolution of ~ 0.1 μHz. We have repeated the procedure described above and determined the periods and amplitudes of each peak. Since the window function of the entire data set is composed of a complex forest of aliases, it was important to extract the frequency components one by one to determine unambiguously the individual components. Again, we found three distinct regions of power in the Fourier transform. Here, we simply summarize the results of our findings in Table 4 for the two dominant modes.

A comparison of the results presented in Tables 3 and 4 indicates that the observed periods have remained constant, within the frequency resolution, during the time span of the observations. The largest difference occurs for the period derived for the $m=-1$ component of the 193 s peak, but it is not significant. The amplitudes, however, seem to have changed slightly over time. Since Table 4 is

TABLE 4. Peaks in the power spectrum obtained from the combined data set.

120 s peak			193 s peak		
Frequency (mHz)	period (s)	Amplitude (%)	Frequency (mHz)	period (s)	Amplitude (%)
8.30596....	120.39543	0.176	5.18702....	192.78879	0.085
8.30869....	120.35585	0.479	5.19000....	192.67841	0.235
8.31124....	120.31905	0.136	5.19282....	192.57373	0.191

the *combined* result of all runs, the amplitudes of each frequency component during the early Mount Bigelow runs could have been relatively different from those determined during the WET campaign. This may indicate that some energy has been transferred between modes with different m values or, alternatively, that there are some unresolved or undetected pulsation modes in the period structure of each peak. If the latter explanation is correct, the spherical harmonic index could be larger than $l=1$ for each peak.

The suggestion that the amplitudes of the frequency components within a peak may vary is in contrast with what was observed by Kepler *et al.* (1983) in another ZZ Ceti star, G226−29, where it was determined that the observed mode near 109 s was composed of a closely spaced triplet whose periods, phases, and particularly amplitudes were strictly constant over time. Furthermore, they showed that the beating observed in the light curve was consistent with that obtained from combining the individual frequency components together. Another well-observed ZZ Ceti pulsator with a very stable period structure is L19−2 (O'Donoghue & Warner 1987). In the following, we consider all the observations presented in this paper to investigate quantitatively the amplitude variation of each dominant mode as a function of time, and to assess whether or not this variation is consistent with beating of three closely-spaced frequency components with constant amplitudes.

Figure 9 illustrates the amplitudes of the 120 and 193 s peaks (as determined from the Fourier transform of the individual runs) as a function of time during the WET campaign. Figure 10 displays the same information for the Mount Bigelow and CFHT runs. The zero point for the time has been set arbitrarily just before the beginning of the WET campaign. One can clearly see the beating in both the 120 and 193 s peaks; the beat periods are approximately 4.4 and 4.1 days for the 120 and 193 s peaks, respectively, a result which is consistent with our earlier estimates. Since the amplitudes of the individual components forming the triplet of each peak are different, it becomes quite cumbersome to attempt to derive an analytical expression for the amplitude modulation as was done, for example, by Kepler *et al.* (1983) for G226−29. Instead, we have explicitly generated synthetic light curves composed of three individ-

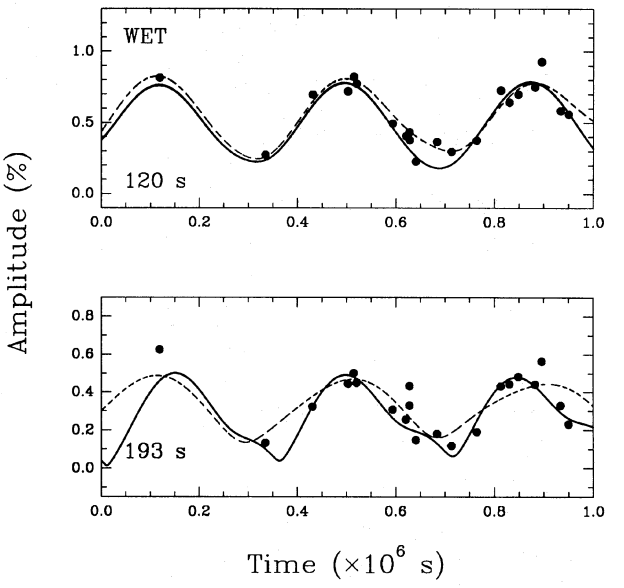

FIG. 9. Amplitude variations of the 120 and 193 s peaks as a function of time during the WET 1990 May campaign. The solid lines indicate the amplitude variation obtain from a combination of the individual frequency components given in Table 4. The dashed lines represent our best fit to the data under the assumption that only three individual components are present (see text).

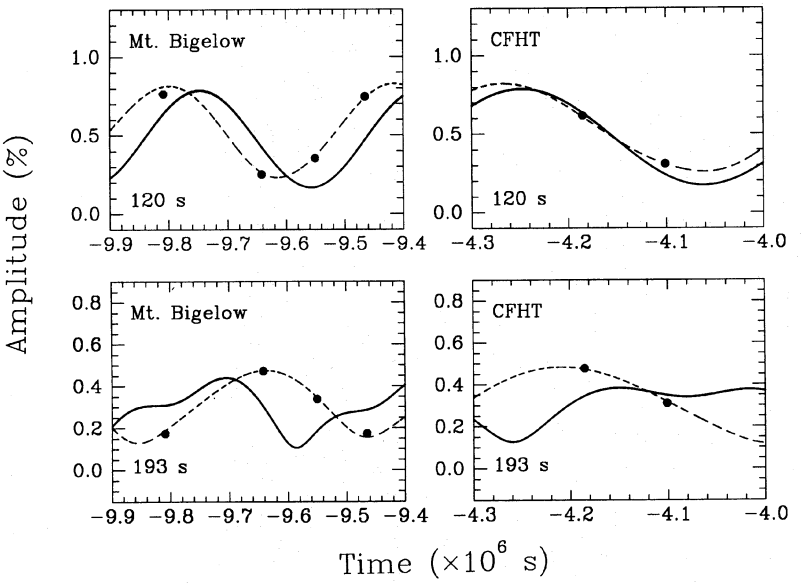

FIG. 10. Same as Fig. 9 but for the Mount Bigelow and CFHT runs.

TABLE 5. Periods and amplitudes required to reproduce the observed amplitude modulations.

120 s Peak			193 s Peak		
Frequency (mHz)	Period (s)	Amplitude (%)	Frequency (mHz)	Period (s)	Amplitude (%)
8.30597....	120.39537	0.104	5.18758....	192.76824	0.036
8.30870....	120.35572	0.521	5.18984....	192.68418	0.302
8.31122....	120.31932	0.208	5.19240....	192.58912	0.364

ual components with known amplitudes, periods, and phases, and derived the amplitude modulations by simply connecting the peaks at maximum amplitude. If we use the values of the amplitudes and periods given in Table 4 as well as the inferred phases, we obtain the results presented in Figs. 9 and 10 as solid curves. The 120 s peak modulation is fairly well reproduced, except for a significant and puzzling systematic shift present in the Mount Bigelow data; the beat period seems consistent, however. On the other hand, the 193 s peak modulation is inconsistent with the results of Table 4, except perhaps during the WET campaign.

We have calculated also the periods, amplitudes, and phases (considered as free parameters) of the three individual components *required* to reproduce the observed modulations; in doing so, we have given equal weight to each data set. Our results are shown as dashed curves in Figs. 9 and 10, and summarized in Table 5. For the 120 s peak, we find that it is possible to reproduce the observed modulation with three components whose periods are in good agreement with the values given in Table 4, but with different amplitudes. This is in line with the conclusion reached above that the periods have remained constant over time, but that the amplitudes of each component may have varied. For the 193 s period, it is still possible to reproduce the modulation with only three components, but the derived amplitudes are completely inconsistent with the values given in Table 4, and even the inferred periods appear to differ from the observed periods more than should be permitted by the resolution. Therefore, from the analysis of the amplitude modulation and the period structure of the Fourier transforms, we conclude that either (1) the 120 and 193 s peaks cannot be decomposed into three components whose amplitudes (and periods and phases) are constant over time, or (2) that there are a number of unresolved components whose amplitudes are small and undetected.

Improved values for the frequency spacings can be obtained from the results of Table 4. Since these values have a higher accuracy (because of the frequency resolution) than those obtained from the WET data set alone, the spacings can ultimately be used to constrain better the mode identification. From Table 4 we obtain $\delta\nu_{m=+1,0}=2.55$ μHz and $\delta\nu_{m=0,-1}=2.73$ μHz for the 120 s peak, and $\delta\nu_{m=+1,0}=2.82$ μHz and $\delta\nu_{m=0,-1}=2.98$ μHz for the 193 s peak. Since the resolution is ~ 0.1 μHz, these results are marginally consistent with an equal frequency spacing within each peak, although the small observed asymmetry could be real as well. We note in this respect that the frequency difference between the central component ($m=0$) and the retrograde mode ($m=-1$) appears to be larger than the spacing between the $m=0$ and $m=+1$ components, as observed in the well-studied object L19−2 (O'Donoghue & Warner 1982, 1987). Again, however, we must be careful against overinterpreting these apparently asymmetric frequency spacings. If we take the average values, we obtain $\delta\nu_{\Delta m=1}=2.64$ μHz and $\delta\nu_{\Delta m=1}=2.90$ μHz for the 120 and 193 s peaks, respectively. These two values are significantly different and confirm our earlier suspicion (Sec. 4) that the low-order modes observed in GD 165 do not have the same rotationally-induced frequency splittings. Unlike the case of the hot pulsating pre-white dwarf PG 1159−035 (for which *asymptotic* pulsation theory has been so successfully used; Winget *et al.* 1991), the low orders of the modes in GD 165 prevent us from inferring directly a rotation period from the observed frequency splittings. Given that the rotation coefficients depend on both k and l for low-order modes (Brassard *et al.* 1992) and in the absence of specific identifications, we can only estimate a rotation time scale. We find $T\sim(2.77\ \text{mHz})^{-1}\sim 4.2$ days, where we have taken the average of the spacings for the 120 and 193 s modes. This characteristic rotation timescale is compatible with the observed beat periods alluded previously.

Finally, we comment on the structure of the two dominant multiplets detected in GD 165. The observations reported here certainly suggest that the 120 s pulsation is composed of at least three frequency components (although the case for five components cannot be totally excluded; see Fig. 7). As is well known, if the *a priori* assumption is made that all the m frequency components of a multiplet are equally excited in a star, then the relative *observed* amplitudes of the components reveal the angle i between the line of sight and the axis of symmetry of the pulsation (presumed to be also the rotation axis). In such a case, the components with the same value of $|m|$ have the same amplitudes, leading to a multiplet which has a symmetric structure about the central component ($m=0$). Disregarding for the moment the fact that the two side components of the central 120.35585 s peak in the Fourier spectrum do not have exactly the same amplitudes, it is possible to find values of i which could explain, by simple geometric effects, the fine structure of the 120 s mode (Pesnell 1985; Brassard *et al.* 1993b). Thus, if the 120 s

pulsation is a triplet ($l=1$) produced by rotation splitting, a value of $i \simeq 23°$ could account for the relative amplitudes of the three components (we have assumed here that the two $|m|=1$ components have the same amplitudes obtained by averaging the individual values in Tables 3 and 4). Likewise, if the 120 s mode were a quintuplet ($l=2$), an inclination angle of $i \simeq 12°$ could account for the observed structure of the multiplet, including very small $|m|=2$ components which could correspond to the two small peaks indicated by short tick marks in Fig. 7.

The approximate symmetry about the central component observed in the 120 s complex is definitely not present in the 193 s multiplet. It is not even clear at the present whether or not we can really assign a value of $m=0$ to the largest amplitude component with the period 192.67841 s. If one does assign that value, then the observed structure is not symmetric about the central component and cannot be explained solely in terms of a simple inclination effect. On the other hand, if one insists on a symmetric pattern, one could imagine that the $m=0$ component is not seen at all and that the two largest components with roughly equal amplitudes in Fig. 8 are side components with the same $|m|$ value. Such a pattern would result from a rotationally-split $l=1$ mode in a pulsator viewed at nearly equator-on position. Since we expect the symmetry axes of the various pulsation modes to coincide, this latter geometry would be incompatible with the one inferred for the 120 s pulsation. Given this incompatibility, given the fact that the two side components of the 120 s peak are not equal in amplitudes, and given the possibility that the amplitude of the components may have changed with time as discussed above, we conclude that the simple geometric effect of a particular viewing angle cannot account for the fine structure of the two dominant modes in GD 165. This behavior has been observed also in other pulsators, and in particular in the hot star PG 1159−035 (see Figs. 5 and 6 of Winget *et al.* 1991). As discussed in that paper, current linear pulsation theory cannot account for such behavior.

6. CONSTRAINTS ON THE HYDROGEN LAYER THICKNESS IN GD 165

The observations described in this paper can profitably be used to constrain the hydrogen layer mass in GD 165, one of the most interesting quantities that can be inferred from white dwarf seismology. The method rests on the combined facts that a sequence of g modes belonging to the same value of l shows a *minimum* period (the period corresponding to the mode with radial order $k=1$), and that the minimum period is quite sensitive to stellar parameters, in particular the total mass and hydrogen layer mass in ZZ Ceti star models (see, e.g., Brassard *et al.* 1992). If a pulsator shows an excited mode with a period short enough to make it sensitive to these stellar parameters, then one can hope to constrain them. This method was applied successfully by Fontaine *et al.* (1992) to the ZZ Ceti star G226−29, a pulsator showing a single region of power in its Fourier spectrum consisting of a well-defined triplet centered on a period of ~109 s (Kepler *et al.* 1983). By combining new period data obtained from the recent adiabatic survey by Brassard *et al.* (1992) with new spectroscopic determinations of atmospheric parameters of G226−29, Fontaine *et al.* (1992) found that it must have a relatively thick hydrogen layer of $\log q(\mathrm{H}) \equiv \log[\mathcal{M}(\mathrm{H})/\mathcal{M}_*] = -4.4 \pm 0.2$ if, as suggested by the triplet structure of the 109 s peak in the Fourier transform domain, the observed pulsations correspond to an $l=1$ mode.

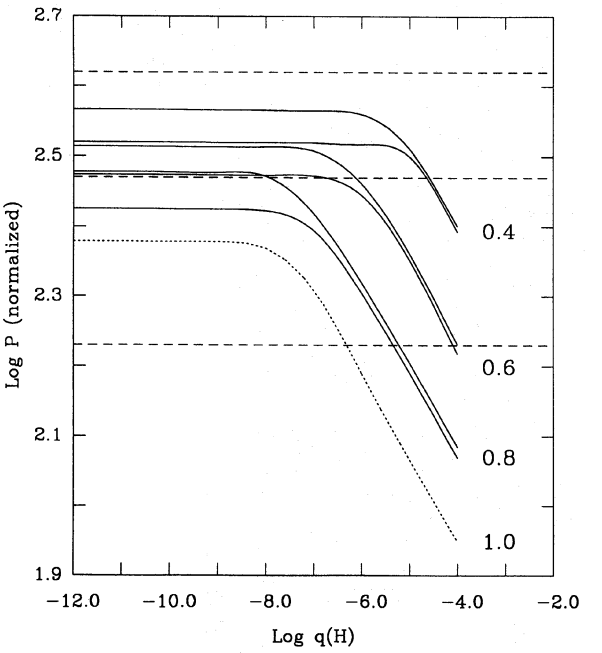

FIG. 11. Normalized period, $\sqrt{l(l+1)}P_{1l}$ of the $k=1$ mode as a function of the fractional hydrogen layer mass for DA models with different masses and effective temperatures (continuous and dotted curves). In comparison, the dashed horizontal lines give the normalized periods for the observed 120 s pulsation in GD 165 assuming that the mode has $l=1$ (lower line), $l=1$ (middle line), and $l=3$ (upper line).

The period of the 120 s mode in GD 165 is sufficiently short that an analysis similar to that of Fontaine *et al.* (1992) for G226−29 can be carried out. Hence, in Fig. 11, the three horizontal dashed curves correspond, from top to bottom, to the normalized period ($\sqrt{l(l+1)}P$) of the 120 s mode assuming that it has a value of $l=3$, 2, and 1, respectively. In comparison, the three sets of two continuous curves give the expected normalized periods of the g mode with the shortest period (e.g., $k=1$) as functions of the hydrogen layer fractional mass for models with masses $\mathcal{M}/\mathcal{M}_\odot=0.4$, 0.6, and 0.8. The dotted line refers to the expected periods for models with $\mathcal{M}/\mathcal{M}_\odot=1.0$ and $T_{\rm eff}=14\,000$ K, as based on an extrapolation of the results of Brassard *et al.* (1992) to a higher mass. In terms of the

normalized periods, Fig. 11 could be considered as a "universal" diagram, valid for any value of l. For each set, the lower curve corresponds to models with $T_{\rm eff}=14\,000$ K, while the upper curve corresponds to models with $T_{\rm eff}=12\,000$ K. This illustrates the (small) effects of changing the effective temperature. Note as well that the period of a g mode with $k=1$ is the *smallest* possible for a sequence of a given l value, so that inferences about the hydrogen layer mass will correspond to *lower* limits if the 120 s mode turns out to have $k>1$.

We have used the spectroscopic method of Bergeron *et al.* (1992a) supplemented by the recent results of Bergeron *et al.* (1991, 1992b) in conjunction with new high signal-to-noise spectroscopic observations to derive the atmospheric parameters of GD 165. Our best estimates give $T_{\rm eff}=13\,300\pm200$ K and $\log g=7.96\pm0.05$, the latter corresponding to a mass $\mathcal{M}/\mathcal{M}_{\odot}=0.56\pm0.03$ according to the evolutionary models of Wood (1990). Using these parameters, we find from Fig. 11 that the hydrogen layer mass in GD 165 is $\log q({\rm H})\approx-3.7\pm0.2$ (or larger if $k>1$) if the 120 s pulsation is an $l=1$ mode. Likewise, we find that $\log q({\rm H})\approx-6.4\pm0.2$ if, in contrast, the 120 s pulsation is an $l=2$ mode. No useful constraint on the hydrogen layer mass can be obtained from period data if the observed mode turns out to have a spherical harmonic index $l=3$. This last possibility cannot totally be ruled out, but is not favored on the grounds that it would require rather large temperature perturbations to account for the observed luminosity variations (Brassard *et al.* 1993b).

We note that the solution for $l=1$ suggests a hydrogen layer mass which tends to be uncomfortably large for a white dwarf (D'Antona & Mazzitelli 1979). This may be taken as circumstantial evidence against the $l=1$ identification, although this evidence is rather weak, at best. Unfortunately, the results of the present analysis do not allow us to decide on the issue. As shown in Fig. 7, the structures identified by long tick marks are associated with three individual frequency components, and are interpreted as an $l=1$ mode split by slow rotation. The discussion presented in Sec. 5, however, also suggests that the choice $l=2$ remains possible.

7. CONCLUSION

The observations presented in this paper amount to some 103 h of white light photometry on GD 165. We have studied the star at an unprecedented level of sensitivity (with the CFHT) and at an unprecedented temporal resolution (with the WET network). These results have already permitted us to make significant progress toward a detailed understanding of the physical structure of GD 165.

We point out in this context that, despite the fact that the details of the evolution of a cooled down white dwarf such as a ZZ Ceti star are much more secure than those of a hot PG 1159 star, the seismological information contained in the pulsations of a ZZ Ceti star is much sparser and more difficult to interpret. Indeed, many modes tend to be excited simultaneously in a PG 1159 pulsator, while generally, a ZZ Ceti star tends to be quite selective in the number and type of modes it chooses to excite. Also, the observed modes in PG 1159 objects are generally high order modes, for which the simple but powerful tools of *asymptotic* pulsation theory can be used. We cannot afford this luxury for ZZ Ceti pulsators, as most of the modes of interest are low-order modes for which asymptotic theory does not apply. For example, rotation periods can readily be estimated from observed frequency splittings in the appropriate limit of high-order modes when the rotation coefficient becomes independent of the radial order k. In contrast, for low-order modes such as those observed in GD 165, the rotation coefficient depends explicitly on the value of k. This implies that the modes must be identified *before* being able to infer a rotation period in a ZZ Ceti star.

Despite these difficulties, we remain quite optimistic about eventually inferring the internal structure of GD 165 through asteroseismological techniques. It would appear, in particular, that high signal-to-noise observations with adequate temporal resolution should further be carried out to exploit the additional information contained in the low-amplitude modes.

We thank Jean S. Ramsay for assistance at the SAAO 0.75 m telescope on 1990 May 27–28. This work was supported in part by the NSERC Canada, and by the Fund FCAR (Québec). T.A. acknowledges support by the Netherlands Foundation for Research in Astronomy (NFRA) with financial aid from the Netherlands Organization for Scientific Research (NWO) under Contract No. 782-371-038. J.T.M. acknowledges the support of NSF Grant No. 88-00298. We are grateful to the Director, the Time Allocation Committee, and the staff of the CFHT for their support, and to the Director and the staff of the SAAO for the continuing support of WET runs.

REFERENCES

Bergeron, P., & McGraw, J. T. 1990, ApJ, 352, L45
Bergeron, P., Saffer, R. A., & Liebert, J. 1992a, ApJ, 394, 228
Bergeron, P., Wesemael, F., & Fontaine, G. 1991, ApJ, 367, 253
Bergeron, P., Wesemael, F., & Fontaine, G. 1992b, ApJ, 387, 288
Brassard, P., Fontaine, G., Wesemael, F., & Talon, A. 1993a, in White Dwarfs: Advances in Observation and Theory, edited by M. A. Barstow (NATO ASI Series), p. 485
Brassard, P., Fontaine, G., Wesemael, F., & Tassoul, M. 1992, ApJS, 81, 747
Brassard, P., Wesemael, F., & Fontaine, G. 1993b, in preparation
D'Antona, F., & Mazzitelli, I. 1979, A&A, 74, 161
Daou, D., Wesemael, F., Bergeron, P., Fontaine, G., & Holberg, J. B. 1990, ApJ, 364, 242
Fontaine, G., Bergeron, P., Vauclair, G., Brassard, P. Wesemael, F., Kawaler, S. D., Grauer, A. D., & Winget, D. E. 1991, ApJ, 378, L49
Fontaine, G., Brassard, P., Bergeron, P., & Wesemael, F. 1992, ApJ, 399, L91
Kepler, S. O., *et al.* 1991, ApJ, 378, L45
Kepler, S. O., Robinson, E. L., & Nather, R. E. 1983, ApJ, 271, 744
Nather, R. E. 1989, in White Dwarfs, IAU Colloquium No. 114, edited

by G. Wegner (Springer, New York), p. 305
Nather, R. E., Winget, D. E., Clemens, J. C., Hansen, C. J., & Hine, B. P. 1990, ApJ, 361, 309
O'Donoghue, D., & Warner, B. 1982, MNRAS, 136, 293
O'Donoghue, D., & Warner, B. 1987, MNRAS, 228, 949
Pesnell, W. D. 1985, ApJ, 292, 238
Unno, W., Osaki, Y., Ando, H., Saio, H., & Shibahashi, H. 1989, Nonradial Oscillations of Stars (University of Tokyo Press, Tokyo)
Winget, D. E. 1991, in 7th European Workshop on White Dwarfs, edited by G. Vauclair and E. M. Sion (NATO ASI Series), p. 159
Winget, D. E., *et al.* 1990, ApJ, 357, 630
Winget, D. E., *et al.* 1991, ApJ, 378, 326
Winget, D. E., & Fontaine, G. 1982, in Pulsations in Classical and Cataclysmic Variable Stars, edited by J. P. Cox and C. J. Hansen (University of Colorado, Boulder), p. 46
Wood, M. A. 1990, Ph.D. thesis, University of Texas at Austin